On the efficiency of dual-chamber biocatalytic electrochemical cells applying membrane separators prepared with imidazolium-type ionic liquids containing [NTf$_2$]$^-$ and [PF$_6$]$^-$ anions

László Koók[1], Nándor Nemestóthy[1], Péter Bakonyi[1], Attila Göllei[2], Tamás Rózsenberszki[1], Piroska Takács[1], Alexandra Salekovics[1], Gopalakrishnan Kumar[3,*], Katalin Bélafi-Bakó[1]

[1]Research Institute on Bioengineering, Membrane Technology and Energetics, University of Pannonia, Egyetem ut 10, 8200 Veszprém, Hungary

[2]Department of Electrical Engineering and Information Systems, University of Pannonia, Egyetem ut 10, 8200 Veszprém, Hungary

[3]Green Processing, Bioremediation and Alternative Energies Research Group, Faculty of Environment and Labour Safety, Ton Duc Thang University, Ho Chi Minh City, Vietnam

Email: gopalakrishnankumar@tdt.edu.vn

[*]Corresponding Author at : Dr. Gopalakrishnan Kumar , Green Processing, Bioremediation and Alternative Energies Research Group, Faculty of Environment and Labour Safety, Ton Duc Thang University, Ho Chi Minh City, Vietnam, E-mail: gopalakrishnankumar@tdt.edu.vn

Abstract

In this study, the dependency of energy recovery on separator characteristics applied in microbial fuel cells (MFCs) was sought by testing an emerging class of membranes (supported ionic liquid membranes (SILMs), prepared with [hmim][PF$_6$] and [bmim][NTf$_2$] ionic liquids) comparatively with well-known proton exchange (Nafion N115) and microfiltration (PVDF) counterparts. Crucial membrane features such as O$_2$ and substrate (acetate as the sole carbon source) crossovers were assessed and as a result, mass transfer as well as diffusivity coefficients of these compounds (k_O, k_A, D_O, D_A, respectively) were determined. The experiments showed that SILM-operated MFCs could work in a reliable way and among them, the [bmim][NTf$_2$]-based one produced higher specific energy yield (Y_S = 9.78 kJ g^{-1}$_{CODin}$ m^{-2}) than the Nafion-MFC (Y_S = 8.25 kJ g^{-1}$_{CODin}$ m^{-2}) used as an important reference. This outcome was found to be associated with the membrane-cross oxygen shuttle properties of the membranes (k_O = 1.25 cm s^{-1} and 1.31 cm s^{-1}, respectively). As for the two SILMs, significant differences in terms of the energy yield, mass transfer and diffusion coefficients were noted, however, it has appeared from cell polarization measurements that the internal resistances of the SILM-MFCs were nearly the same. The evaluation of the SILM-operated MFCs' power production was complemented by measuring the dielectric traits of ionic liquids that can be related with the ion conductivity of these materials. It turned out that the [hmim][PF$_6$] IL had an order of magnitude lower ionic conductivity.

Keywords: bioelectrochemical system, microbial fuel cell, membrane, ionic liquid, substrate crossover, oxygen mass transfer

1. Introduction

Microbial fuel cells (MFC) are rapidly evolving applications in field of the microbial electrochemical systems that have attracted notable attention in the past decade. MFCs have the capability to convert chemical energy – bound in the wide range of organic matters – to electricity directly by the aid of electro-active microorganisms [1,2]. Attributed to this potential, there has been an ongoing and still increasing trend in the deployment of MFC devices for the treatment of wastewaters, making concurrent energy recovery possible. Until recently, a variety of (i) real i.e. landfill-derived waste liquor [3] as well as (ii) synthetic wastewaters containing relatively simple compounds i.e. glucose, acetate, alcohols, volatile fatty acids, etc. were exploited with success in MFCs [4]. It is noteworthy however that to achieve cost-effective and low-energy demand utilization of waste streams in MFCs, further understanding and improvement of key-areas in the design of the whole equipment are required [5]. In this concern, besides the biological component of the bioelectrochemical reactor (associated primarily with the active, exo-electrogen biofilm coating the anode), system architecture should also be considered carefully [6].

From this latter point of view, the *membrane* (as a solid, ion-conductive electrolyte) between the anode and cathode sides is a central element of the traditional, two-chamber MFCs. It plays a critical role in sustaining the transport of protons to complete the half-cell reaction on the cathode ($O_2 + 4e^- + 4H^+ = 2\ H_2O$), where molecular oxygen gas is normally supplied from air,

meanwhile the electrons reaching the cathode (via external wiring) are liberated from organic matter decomposition, taking place in the anode half-cell and catalyzed by the exo-electrogen bacteria [7]. Furthermore, to enhance power generation and Coulombic efficiency (*CE*) of dual-chamber MFC, an ideal membrane ought to reflect certain essential properties. For instance, it is preferably made of a material that ensures fast (and selective) proton transfer [8], has low permeability to O_2 [9], decreases the level of pH splitting (meaning the formation of pH gradient between anode and cathode half-cells) [10], prevents substrate i.e. acetate crossover [11], characterized with small ohmic resistance [12], withstands biofouling [13] and is affordable.

So far, the ion, in particular proton exchange membranes (PEM) such as Nafion have been the most often employed separators for laboratory-scale MFC research [14]. However, according to various reports, there is a broad consent in the literature that Nafion fails to meet all the criteria referred above since besides its considerable price, notable O_2 transport has been observed for this polymer [15,16].

Such features have fostered the engineering of membrane separators to be applied in MFCs and as a result, alternative materials including ceramics [17], functionalized composites [18], cheaper, conventional (i.e. polypropylene) as well as designer (i.e. sulfonated polystyrene-ethylene-butylene-polystyrene) polymers [19,20], ultra- and microfiltration membranes [21,22] have been spotlighted. Additionally, the research line has just lately been expended with

the development of membranes synthetized and prepared with ionic liquids (IL) [23,24].

A highlight (brief literature survey) on the advantages and use of ILs in MFCs was given in our recently published paper [25], where the performance of MFCs operated with membranes containing [bmim][NTf$_2$] and [hmim][PF$_6$] ILs was evaluated comparatively to Nafion-MFC. It was shown that actual, specific energy gains from substrates i.e. glucose and acetate were dependent on the membrane type. However, no clear explanation could be provided to elucidate the MFC behaviors in the presence of different separators [25], encouraging further investigation on the topic.

Therefore, this is a follow-up study being in our research sequence on bioelectrochemical systems and its added-value (compared to previous investigations) is the throughout elaboration of cell performance (energy yield, denoted with Y_S) in the light of substantial membrane properties (O$_2$ transfer and substrate crossover) and dielectric traits of ILs ([bmim][NTf$_2$] and [hmim][PF$_6$]). To our knowledge, such analysis with these membranes has not been performed before. Consequently, the results can have sufficient scientific contribution on international grounds and may facilitate the development of wastewater-MFCs for improved treatment efficacy.

2. Materials and Methods

2.1. SILM preparation

The SILMs were fabricated by immobilizing imidazolium-type ionic liquids – (i) 1-butyl-3-methylimidazolium bis{(trifluoromethyl)sulfonyl}imide ([bmim][NTf$_2$]) and (ii) 1-hexyl-3-methylimidazoluim hexafluorophosphate ([hmim][PF$_6$]) (products of IoLiTec, Germany, 99% purity) – in (the pores of) hydrophobic Durapore PVDF (Sigma-Aldrich, USA) microfiltration support layer. As for the ILs' structures, the [NTf$_2$]$^-$ anion is more water immiscible than [PF$_6$]$^-$ and therefore, the counter cation of [PF$_6$]$^-$ was chosen to be a longer alkyl chain ([hmim]$^+$ against [bmim]$^+$) [26], balancing the final hydrophobicities to be comparable levels. More details on the procedure of SILM preparation are described in our earlier publications [25].

2.2. MFC setup

In this study, the basic design of two-chambered MFCs was adopted from our previous work [25]. In brief, the anode half-cell (60 mL total capacity) contained a piece of carbon cloth (64 cm^2 apparent surface area) (Zoltek Corp., USA) – connected by titanium wiring (Sigma-Aldrich, USA) to the electric circuit – as anode to be colonized by the exo-electrogen strains (supplied from mesophilic anaerobic sludge as inoculum). In the continuously

aerated cathode chamber, another piece of carbon cloth (similar to the one in the anode compartment) was fixed on Ti wire as cathode to ensure electrical connection. A 100 Ω resistor was placed in the external circuit to monitor the potential difference between the anode and cathode. The catolyte was 50 mM phosphate buffer with pH=7. In the anode side, synthetic wastewater with pH adjusted to 7 was filled, comprising of Na-acetate as the sole carbon source [16]. The half-cells were separated either by Nafion N115 (Sigma-Aldrich, USA), Durapore PVDF or the SILMs prepared (Section 2.1.). All were cut to circle shape with 4.5 cm diameters. Before use, the Nafion was activated by following the same method as in our earlier paper [25]. More details on start-up and subsequent operation will be discussed in Section 3.1. The MFCs were running under constant temperature conditions (35 ºC) and purged with high-purity N_2 in the beginning to remove dissolved oxygen from the anode chamber. In general, the results presented later on related to our various MFCs (Section 3.) are mean values from duplicate experiments.

2.3. Analysis and Calculations

The voltage difference between the anode and cathode electrodes was recorded by a DAQ (National Instruments, USA). In accordance with Ohm's law, current and other electrical data (i.e. electric power) were computed. The energy yield (Y_S) was delivered by Eq. 1:

$$Y_S = \frac{\int_0^\tau P(t)dt}{m(COD_{in})\, A} \tag{1}$$

where P is the electric power (W), A is the apparent anode surface area (m^{-2}), τ is the operation time (h) for a batch MFC cycle and $m_{(CODin)}$ is the quantity of COD (grams) supplied with acetate in the synthetic wastewater during a given cycle.

To conduct cell polarization, resistors in the external electric circuit of the MFCs were varied in the range of 10 Ω – 3.3 kΩ. From the linear region of the polarization curves acquired, the overall internal cell resistance (R_i) could be derived as the slope of the fitted trendline (**Table 1**).

For all the four membranes, the determination of individual mass transfer features (k_O, k_A, D_O, D_A) was carried out in an abiotic MFC (lacking the bioanode, but equipped with dissolved oxygen sensor in the anode chamber) by complying the procedure and calculations described in the article of Kim et al. [27]. k_O and k_A are the mass transfer coefficients of oxygen and acetate, respectively. D_O and D_A represent the diffusivity of the same substances, respectively.

To measure the dielectric properties of the two ILs, an equipment – designed and built at University of Pannonia, Hungary – based on the compensation of the phase change in the liquid sample as response to the absorption of microwave energy was used. The test rig contains a sample holder, thermostat, peristaltic pump, displaceable piston, stepper motor, magnetron, detectors, sensors and control unit. In the device, the liquid

sample is circulated and the energy is provided by the magnetron in form of microwaves. The returning waves can be analyzed by four detectors on a personal computer. More details about the apparatus and method can be found in the publication by Göllei et al. [28].

The dielectric permittivity (ε) establishes a relationship between the charge motion in dielectrics caused by the external electrical field and the resulting charge distribution, and can be expressed by Eq. 2 [29].

$$\varepsilon = \varepsilon' \text{-} j\varepsilon'' \tag{2}$$

where ε' is the dielectric constant, ε'' is the dielectric loss factor and $j = \sqrt{-1}$ is the complex unit. In dielectrics, the dielectric loss factor is proportional to the ionic conductivity according to Eq. 3 (assuming that the dipole rotation is negligible relative to the ionic conduction) [29].

$$\varepsilon'' = \frac{\sigma}{\varepsilon_0 \omega} \tag{3}$$

where σ is the ionic conductivity of the dielectric, ε_0 is the vacuum permittivity and ω is the angular frequency. The classification of materials based on their ε value can be made by calculating the so-called loss tangent, $\tan(\delta)$ in Eq. 4:

$$\tan(\delta) = \frac{\varepsilon''}{\varepsilon'} \tag{4}$$

3. Results and Discussion

3.1. Performance evaluation of MFCs using various membrane separators

The SILMs were prepared with average ionic liquid content of 11.4 g cm^{-2} (relative to the membrane surface area), which is highly comparable to that reported in our recent work [25]. Firstly, the MFCs operated with the four different membranes (Nafion, PVDF, [bmim][NTf$_2$]-SILM, [hmim][PF$_6$]-SILM) were acclimatized by ensuring 5 mM acetate (in the anolyte solution) during batches, repeated as long as the currents became stabilized at least for 3 successive cycles. At this point, the anode acclimation period was considered finished. Afterwards, investigating the membrane-related effects on the MFC performance was commenced.

Under stabilized MFC operation, the Nafion-MFC and [bmim][NTf$_2$]-MFC produced nearly equal voltage (20.8 and 20 mV at the voltage curve plateau, respectively) as response to 5 mM acetate supplied during the batch cycles. This corresponds to current- and power densities of 32.5 mA m^{-2}, 31.3 mA m^{-2} and 0.68 mW m^{-2}, 0.63 mW m^{-2}, respectively. From the former aspect, somewhat weaker results were attained with the [hmim][PF$_6$]-MFC and PVDF-MFC (19.4 and 17.2 mA m^{-2}, respectively). These values are comparable to those found in the relevant literature, where for instance Ieropoulos et al. [30] communicated 1.17 – 5.93 mA m^{-2} current and 0.257 – 1.175 mW m^{-2} power densities by acetate-utilizing (5 mM) Nafion-MFCs inoculated by *G.*

sulfurreducens. Furthermore, Chaudhuri and Lovley [31] reported 28-74 mA m^{-2} current densities for glucose-fed MFCs equipped with graphite anodes and Nafion membrane separator. Besides, Hernández-Fernández et al. [24] demonstrated volume specific power density data in the range of 60 – 200 mW m^{-3} by using wastewater-MFC installed with Nafion PEM, [omim][NTf$_2$] and [omim][PF$_6$]-based nylon SILMs. In our present work, power densities ranged between 20 – 72 mW m^{-3}. Though these data agree well and are in the same order of magnitude, it has turned out in this study that the [NTf$_2$]$^-$ anion containing SILM generated 2.6-times higher value in comparison with the one carrying the [PF$_6$]$^-$, while the opposite trend was observed by Hernández-Fernández et al. [24] . This discrepancy may be ascribed to the use of ionic liquids possessing various structure in terms of the cations ([omim]$^+$ thoroughly in Hernández-Fernández et al. [24] and either [bmim]$^+$ or [hmim]$^+$ in the current examination). Moreover, other differences in the experimental circumstances such as the immobilization matrices (nylon by Hernández-Fernández et al. [24] vs. PVDF here) could have also some contribution.

From the energy yields' point of view, the [bmim][NTf$_2$]-MFC produced the highest value with 9.78 kJ g$^{-1}_{CODin}$ m^{-2}, exceeding by ~18 % the one observed for Nafion-MFC (Y_S = 8.25 kJ g$^{-1}_{CODin}$ m^{-2}). In comparison, the [hmim][PF$_6$]-MFC and the PVDF-MFC were less attractive by demonstrating only 2.52 kJ g$^{-1}_{CODin}$ m^{-2} and 2.43 kJ g$^{-1}_{CODin}$ m^{-2}, respectively. Basically, these performances coincide with those in our previous work [25].

For the record, the fact that MFCs designed with the SILMs were able to run efficiently for a longer period of time (through multiple batch cycles, similarly to those MFCs put to operation with the Nafion or PVDF membranes) is a good indication that the ILs did not take an observable negative effect on the stability of the bioelectrochemical application [25].

3.2. *Cell polarization and MFC internal resistance*

After leaving the start-up phase of MFCs behind, cell polarization measurements were carried out and the voltage output as a function of the external resistance was recorded. The polarization curves of the MFCs working with a particular membrane can be seen in **Fig. 1**, where it is to conclude that Nafion-MFC produced the highest current density by reaching 70 mA m^{-2}. In contrast, the [bmim][NTf$_2$]-MFC peaked at 35 mA m^{-2}, followed by the PVDF-MFC (31 mA m^{-2}) and the [hmim][PF$_6$]-MFC (30.8 mA m^{-2}). Additionally, it can be inferred from **Fig. 2** that after reaching a limiting current density, a phenomenon so-called power overshoot occurred, being the most pronounced in case of [hmim][PF$_6$]-MFC.

Considering the maximal power density data, it can be said that with 12.2 mW m^{-2} the Nafion-MFC demonstrated a roughly three-times higher $P_{d,max}$ than the other MFCs (**Fig. 2**). From the appropriate analysis of polarization curves, the total internal resistance of the biological fuel cells was estimated. As a matter of fact, the R_i values obtained were 1.35 kΩ, 2.56 kΩ, 2.88 kΩ and

4.56 kΩ for the Nafion-MFC, [bmim][NTf$_2$]-MFC, [hmim][PF$_6$]-MFC and PVDF-MFC, respectively (**Table 1**). In the already published literature, Ieropoulos et al. [30] reported 1.1 kΩ internal resistance for Nafion-MFCs using acetate substrate, which fairly matches with our value for this type of membrane. In addition, the research of Oh and Logan [32] showed internal resistance values for Nafion-MFCs between 89 Ω – 1.1 kΩ (depending on the membrane size), which agrees well with our relevant data obtained. Actually, literature information concerning R_i in MFCs using IL-membrane as separator is quite limited. In a research paper by Hernández-Fernández et al. [23] it was confirmed that polymer inclusion ionic liquid membranes (PIILMs) are capable to function as separators of electrode chambers in MFC treating wastewater. In essence, by using PVC as polymer, they prepared [omim][PF$_6$] and [mtoa][Cl]-based PIILMs and obtained 4.5-5.9 kΩ and 0.44-0.75 kΩ internal resistances, respectively. In case of Nafion-MFC (used for benchmarking), R_i of 2.27-2.51 kΩ (double of the one in this work) was noticed.

3.3. *Permittivity measurements of ionic liquids*

Since there was no significant difference between the internal resistances of SILM-MFCs (confirming our previous findings [25]), deeper elaboration of reasons standing behind the distinct MFC performances (described in section 3.1.) was attempted by the practical approach of investigating the specific properties of the ionic liquids used. In this regard, the

scope of interest was set on the ionic conductivity of the ILs, measured through the complex permittivity (Section 2.3.).

It turned out from the results that the [bmim][NTf$_2$] had one order of magnitude higher ionic conductivity (σ = 283.5 mS m^{-1}) than [hmim][PF$_6$] (σ = 21.8 mS m^{-1}), as highlighted in **Table 1**. By taking into consideration the tan(δ) values, it can be deduced that while [hmim][PF$_6$] is a poorly-conductive IL (in other words, a good dielectric), the [bmim][NTf$_2$] may be viewed as a lossy conducting ionic liquid, as tan(δ) approximates to 1 [33].

In conclusion, [bmim][NTf$_2$] seems to be a more efficient ionic conductor than [hmim][PF$_6$], which would appear to be useful in pushing the MFC towards more attractive energy yields. Nevertheless, more research and feedback is encouraged in this aspect.

3.4. Assessing O$_2$ and acetate mass transport characteristics of membranes used in MFCs

The mass transfer and diffusion coefficients for oxygen and acetate were determined in order to compare the four membranes from the standpoint of the transport processes taking place across them in the MFCs (**Table 2**). In fact, remarkable differences in k_O values were noted and accordingly, the membranes could be arranged to the following order: [hmim][PF$_6$]-SILM (15.28 x 10^{-4} cm s^{-1}) > PVDF (2.34 x 10^{-4} cm s^{-1}) > Nafion (1.31 x 10^{-4} cm s^{-1}) > [bmim][NTf$_2$]-SILM (1.25 x 10^{-4} cm s^{-1}). The result for Nafion fits well to

literature data (**Table 2**) where for example, 1.3×10^{-4} cm s^{-1} and 1.4×10^{-4} cm s^{-1} were communicated by Kim et al. [27] and Tang et al. [22], respectively.

Based on the k_O values, we can draw that oxygen was shuttled the most in the MFC by the [hmim][PF$_6$]-SILM, while [bmim][NTf$_2$]-SILM was the least permeable to this substance. This needs more considerations since basically, from the structures of these two ILs, the opposite might be expected. On one hand, the [NTf$_2$]$^-$ anion structure predicts higher oxygen solubility in the IL compared to the [PF$_6$]$^-$ anion [34,35], and moreover, the considerably higher viscosity of [hmim][PF$_6$] implies lower O_2 diffusivity [36]. However, on the other hand, the longer alkyl chain length of the cation ([hmim]$^+$ vs. [bmim]$^+$) would suggest higher gas solubility [37].

Nonetheless, oxygen has basically low solubility in ILs, it interacts weakly with these materials and recent researches showed that the effect of the cation on the solubility and diffusivity of oxygen is quite complex [35,36]. Hence, the results are sometimes contradictory and do not meet the preliminary assumptions, advising that a wider range of ILs' physical properties i.e. free volume is considered [36] to comprehend the underlying phenomena, especially in terms of actual gas solubility/diffusivity in IL systems. In addition, it has to be noted that most of the available data on gas solubility in ILs is associated with CO_2, and information related to O_2 is currently not detailed enough, limiting the understanding of the observations. On the top of that, we suppose that another factor that may strongly affect the gas-IL system is the presence of immobilization support (such as the microfiltration PVDF here). In

this sense, extrapolating from the traits (e.g. solubility and diffusivity) of gases measured separately in ILs to describe the behavior of gas-SILM interactions may be misleading as the solid immobilization phase might cause alterations in these important features of the gaseous compounds.

Regarding the acetate mass transfer and diffusion coefficients, it can be pointed out that Nafion and PVDF separators were the most and least permeable for the substrate, respectively (**Fig. 3**). The low k_A and D_A values for PVDF are in agreement with our preliminary expectations and are probably attributed to the partially gas-filled and blind pores of this hydrophobic microfiltration membrane, obstructing the passage of acetate between the half-cells of MFC. The differences between the chemical structures of Nafion and SILMs are well-reflected in the outcomes. As a matter of fact, the k_A for both IL membranes was significantly lower (0.42×10^{-8} cm s^{-1} and 0.32×10^{-8} cm s^{-1} for [bmim][NTf$_2$]-SILM and [hmim][PF$_6$]-SILM, respectively) than for Nafion (4.35×10^{-8} cm s^{-1}). Although the reasons are not yet fully understood, we can speculate that certain electronic and/or steric hindrances taking place between the acetate molecule and the ionic constituents of the ILs play a role here.

3.5. On the correlation of MFC efficiency with O_2 mass transport through membrane separators

The energy yield (defined in Eq. 1) is an "efficiency-type" parameter and in this sense, it relates with the Coulombic efficiency. Though Y_S and *CE* values are not directly interconvertibles, to certain extent, both measure "how efficiently the substrate fed to the MFC anode is utilized by the electro-active bacteria" and therefore, can serve the evaluation of MFC behaviors on comparative grounds. In **Fig. 4**, the relationship of energy yield and Coulombic efficiency with k_O values is plotted and what we see is that both follow the similar trend. In other words, it is illustrated in **Fig. 4** (based on a sufficient mass of data for various membranes, picked up from **Table 2**) that the Y_S and *CE* are dependent on k_O in the same way.

By dedicating more attention to the discussion of **Fig. 4**, it seems that in the lower k_O range a rapid and sharp fall of both *CE* and Y_S occur along with the increment of k_O. Thereafter, by further enhancement of k_O, the rate of *CE* and Y_S decrease becomes less substantial due to an apparently weaker dependence. This brings a couple of important messages to address.

In the first main region where membranes with low k_O values are found – designated herewith as the *kinetic range* – the change of dissolved oxygen concentration in the anode chamber will interfere the metabolism of the exo-electrogen strains in a proportional manner. In other words, in the *kinetic range*, the portion of electrons consumed for the reduction of O_2 (rather than

being captured by the anode as terminal electron acceptor) is linear-like function of the k_O (and the subsequently occurring, actual dissolved oxygen concentration). The phenomenon that electrons are diverted from the electric circuit leads to the loss of Coulombic efficiency [38] and the obtainable energy yields (related to the decomposition of a given amount of organic matter) is negatively influenced, as well. Furthermore, **Fig. 4** implies a critical k_O, above which the amount of oxygen entering the anode chamber (from the direction of the aerated cathode across the membrane) is excessive and creates therefore highly unfavorable, aerobic conditions and causes strongly deteriorated cell performance. This can be called as the *saturation region* (the place of membranes with k_O higher than the above-referred critical one), where *CE* and *Ys* values are inherently low and vary much less notably with k_O (compared to the *kinetic range*).

To attempt the determination of the critical k_O value (that, by definition, splits the *kinetic and saturation range*s), *CE* vs. k_O data (taken from **Table 2**) were grouped and trendlines were fitted afterwards (inset of **Fig. 4**). As a result, based on the intersection of the two lines appearing in the inset of **Fig. 4**, the critical k_O could be roughly estimated as 1.8×10^{-4} cm s^{-1}. Accordingly, the development and use of membrane separators with a $k_O < 1.8 \times 10^{-4}$ cm s^{-1} seem to be rewarding, which might enable to more adequately diminish losses in dual-chamber MFCs related to the penetration of O_2 to the anaerobic anode half-cell. Nevertheless, to examine with higher accuracy how sharp the transition between the two regions is, further experiments with various

membranes can be proposed that would yield (i) more relevant data and (ii) an increased confidence of analysis.

It is noteworthy despite **Fig. 4** presents that a membrane with k_O approaching to zero (a quasi O_2 impermeable separator) is able to assure high *CE* and Y_S, it must not be forgotten that other operating factors such as the microbial diversity of the inoculum, the biomass growth kinetics, the competition of various (i.e. electrochemically-inactive) strains and concomitant substrate losses, etc. can also affect these efficiency parameters [39]. As a result, the actual MFC performance will be determined by the sum of these (architectural and biological) impacts.

Although a relationship between membrane k_O and the efficiency of the biocatalytic electrochemical cells could be established in **Fig. 4**, further elaboration and understanding of influencing factors for membranes – in particular for those prepared with ILs – can be a way forward and it may be helpful to investigate a summary of literature data (similar to **Fig. 4**) in terms of other parameters (i.e. k_A, permittivity, resistance, etc.), as well. Besides, to address issues that may appear in SILM-MFCs, research on biofouling can be suggested to get an insight to the potential changes in the characteristics of this class of separators, occurring in longer-term operation.

Conclusions

This study investigated the efficiency of dual-compartment microbial fuel cells applying four different membranes. Important properties of the membranes (two of which was prepared either with [bmim][NTf$_2$] or [hmim][PF$_6$] ionic liquids) such as mass transfer and diffusion coefficients of oxygen and acetate were determined. It was found that MFC performances can significantly vary, depending on the type of membrane. In fact, the best energy yield could be achieved with the [bmim][NTf2]-MFC, being actually 18 % higher than for conventional Nafion N115. The correlation of membranes' O$_2$ transport properties with MFC energy efficiency was analyzed by considering our results along with a sufficient number of literature data. As a result, a critical O$_2$ mass transfer coefficient for membrane separators could be suggested, which would assist the maintenance of good MFCs working conditions by reducing losses attributed to (i) the disturbance of anodic electro-active microorganisms as well as (ii) divergence of electrons from the bioelectrochemically-desired metabolism.

Acknowledgement

References

[1] H. Hassan, B. Jin, S. Dai, T. Ma, C. Saint, Chemical impact of catholytes on Bacillus subtilis-catalysed microbial fuel cell performance for degrading 2,4-dichlorophenol, Chem. Eng. J. 301 (2016) 103-114.

[2] A. Sivasankaran, D. Sangeetha, Y.H. Ahn, Nanocomposite membranes based on sulfonated polystyrene ethylene butylene polystyrene (SSEBS) and sulfonated SiO_2 for microbial fuel cell application, Chem. Eng. J. 289 (2016) 442-451.

[3] T. Rózsenberszki, L. Koók, P. Bakonyi, N. Nemestóthy, W. Logrono, M. Pérez M, et al., Municipal waste liquor treatment via bioelectrochemical and fermentation (H_2 + CH_4) processes: Assessment of various technological sequences, Chemosphere 171 (2017) 692-701.

[4] P. Pandey, V.N. Shinde, R.L. Deopurkar, S.P. Kale, S.A. Patil, D. Pant, Recent advances in the use of different substrates in microbial fuel cells toward wastewater treatment and simultaneous energy recovery, Appl. Energy 168 (2016) 706-723.

[5] S.T. Oh, J.R. Kim, G.C. Premier, T.H. Lee, C. Kim, W.T. Sloan, Sustainable wastewater treatment: How might microbial fuel cells contribute, Biotechnol. Adv. 28 (2010) 871-881.

[6] A. Rinaldi, B. Mecheri, V. Garavaglia, S. Licoccia, P.D. Nardo, E. Traversa, Engineering materials and biology to boost performance of microbial fuel cells: a critical review, Energy Environ. Sci. 1 (2008) 417-429.

[7] H. Rismani-Yazdi, S.M. Carver, A.D. Christy, O.H. Tuovinen, Cathodic limitations in microbial fuel cells: An overview, J. Power Sources 180 (2008) 683-694.

[8] X. Zhang, S. Cheng, X. Wang, X. Huang, B.E. Logan, Separator characteristics for increasing performance of microbial fuel cells, Environ. Sci. Technol. 43 (2009) 8456-8461.

[9] M. Oliot, S. Galier, H. Roux de Balmann, A. Bergel, Ion transport in microbial fuel cells: Key roles, theory and critical review, Appl. Energy 183 (2016) 1682-1704.

[10] B.R. Dhar, H.S. Lee, Membranes for bioelectrochemical systems: challenges and research advances, Environ. Technol. 34 (2013) 1751-1764.

[11] J.X. Leong, W.R.W. Daud, K.B. Ghasemi Liew, M. Ismail, Ion exchange membranes as separators in microbial fuel cells for bioenergy conversion: A comprehensive review, Renew. Sustain. Energy Rev. 28 (2013) 575-587.

[12] W.W. Li, G.P. Sheng, X.W. Liu, H.Q. Yu, Recent advances in the separators for microbial fuel cells, Bioresour. Technol. 102 (2011) 244-252.

[13] M. Sun, L.F. Zhai, W.W. Li, H.Q. Yu, Harvest and utilization of chemical energy in wastes by microbial fuel cells, Chem. Soc. Rev. 45 (2016) 2847-2870.

[14] M. Rahimnejad, G. Bakeri, M. Ghasemi, A. Zirepour, A review on the role of proton exchange membrane on the performance of microbial fuel cell, Polym. Adv. Technol. 25 (2014) 1426-1432.

[15] K.J. Chae, M. Choi, F.F. Ajayi, W. Park, I.S. Chang, I.S. Kim, Mass transport through a proton exchange membrane (Nafion) in microbial fuel cells, Energy Fuels 22 (2008) 169-176.

[16] K.Y. Kim, K.J. Chae, M.J. Choi, E.T. Yang, M.H. Hwang, I.S. Kim, High-quality effluent and electricity production from non-CEM based flow-through type microbial fuel cell, Chem. Eng. J. 218 (2013) 19-23.

[17] E. Yang, K.J. Chae, I.S. Kim, Assessment of different ceramic filtration membranes as a separator in microbial fuel cells, Desalin. Water Treat. 57 (2016) 28077-28085.

[18] S. Angioni, L. Millia, G. Bruni, C. Tealdi, P. Mustarelli, E. Quartarone, Improving the performances of Nafion™-based membranes for microbial fuel cells with silica-based, organically-functionalized mesostructured fillers, J. Power Sources 334 (2016) 120-127.

[19] S. Ayyaru, P. Letchoumanane, S. Dharmalingam, A.R. Stanislaus, Performance of sulfonated polystyrene-ethylene-butylene-polystyrene membrane in microbial fuel cell for bioelectricity production, J. Power Sources 217 (2012) 204-208.

[20] S. Kondaveeti, J. Lee, R. Kakarla, H.S. Kim, B. Min, Low-cost separators for enhanced power production and field application of microbial fuel cells (MFCs), Electrochim. Acta 132 (2014) 434-440.

[21] J.R. Kim, S. Cheng, S.E. Oh, B.E. Logan, Power generation using different cation, anion, and ultrafiltration membranes in microbial fuel cells, Environ. Sci. Technol. 41 (2007) 1004-1009.

[22] X. Tang, K. Guo, H. Li, Z. Du, J. Tian, Microfiltration membrane performance in two-chamber microbial fuel cells, Biochem. Eng. J. 52 (2010) 194-198.

[23] F.J. Hernández-Fernández, A.P. de los Ríos, F. Mateo-Ramirez, M.D. Juarez, L.J. Lozano-Blanco, C. Godínez, New application of polymer inclusion membrane based on ionic liquids as proton exchange membrane in microbial fuel cell, Sep. Purif. Technol.160 (2016) 51-58.

[24] F.J. Hernández-Fernández, A.P. de los Ríos, F. Mateo-Ramirez, C. Godínez, L.J. Lozano-Blanco, J.I. Moreno, et al., New application of supported

ionic liquids membranes as proton exchange membranes in microbial fuel cell for waste water treatment, Chem. Eng. J. 279 (2015) 115-119.

[25] L. Koók, N. Nemestóthy, P. Bakonyi, G. Zhen, G. Kumar, X. Lu, et al., Performance evaluation of microbial electrochemical systems operated with Nafion and supported ionic liquid membranes, Chemosphere 175 (2017) 350-355.

[26] P. Wasserscheid, T. Welton, Ionic liquids in synthesis. John Wiley & Sons, 2008.

[27] J.R. Kim, S. Cheng, S.E. Oh, B.E. Logan, Power generation using different cation, anion, and ultrafiltration membranes in microbial fuel cells, Environ. Sci. Technol. 41 (2007) 1004-1009.

[28] A. Göllei, A. Vass, E. Pallai, M. Gerzson, L. Ludányi, J. Mink, Apparatus and method to measure dielectric properties (ε' and ε'') of ionic liquids, Rev. Sci. Instrum. 80 (2009) 044703.

[29] V. Komarov, S. Wang, J. Tang, Permittivity and measurements. Encyclopedia of RF and microwave engineering, John Wiley & Sons, 2005.

[30] I.A. Ieropoulos, J. Greenman, C. Melhuish, J. Hart,Comparative study of three types of microbial fuel cell, Enzyme Microb. Technol. 37 (2005) 238-245.

[31] S.K. Chaudhuri, D.R. Lovley, Electricity generation by direct oxidation of glucose in mediatorless microbial fuel cells, Nat. Biotechnol. 21 (2003) 1229-1232.

[32] S.E. Oh, B.E. Logan, Proton exchange membrane and electrode surface areas as factors that affect power generation in microbial fuel cells, Appl. Microbiol. Biotechnol. 70 (2006) 162-169.

[33] R. Meredith, Engineers' handbook of industrial microwave heating, The Institution of Electrical Engineering, London, United Kingdom, 2009.

[34] J.L. Anderson, J.K. Dixon, J.F. Brennecke, Solubility of CO_2, CH_4, C_2H_6, C_2H_4, O_2, and N_2 in 1-Hexyl-3-methylpyridinium Bis (trifluoromethylsulfonyl) imide: Comparison to Other Ionic Liquids. Accounts Chem. Res. 40 (2007) 1208-1216.

[35] J.L. Anthony, J.L. Anderson, E.J. Maginn, J.F. Brennecke, Anion effects on gas solubility in ionic liquids, J. Phys. Chem. B. 109 (2005) 6366-6374.

[36] A.R. Neale, P. Li, J. Jacquemin, P. Goodrich, S.C. Ball, R.G. Compton, et al., Effect of cation structure on the oxygen solubility and diffusivity in a range of bis {(trifluoromethyl) sulfonyl} imide anion based ionic liquids for lithium–air battery electrolytes, Phys. Chem. Chem. Phys. 18 (2016) 11251-11262.

[37] M Freemantle, An introduction to ionic liquids. Royal Society of Chemistry, 2010.

[38] H. Liu, B.E. Logan, Electricity generation using an air-cathode single chamber microbial fuel cell in the presence and absence of a proton exchange membrane, Environ. Sci. Technol. 38 (2004) 4040-4046.

[39] T.H. Sleutels, L. Darus, H.V. Hamelers, C.J. Buisman, Effect of operational parameters on Coulombic efficiency in bioelectrochemical systems, Bioresour. Technol. 102 (2011) 11172-11176.

[40] B. Hou, J. Sun, Y.Y. Hu, Simultaneous Congo red decolorization and electricity generation in air-cathode single-chamber microbial fuel cell with different microfiltration, ultrafiltration and proton exchange membranes, Bioresour. Technol. 102 (2011) 4433-4438.

Fig. 1 – Polarization curves of Nafion-MFC (♦), [bmim][NTf$_2$]-MFC (△), [hmim][PF$_6$]-MFC (■) and PVDF-MFC (○).

Fig. 2 – Determination of maximal power density in case of Nafion-MFC (♦), [bmim][NTf$_2$]-MFC (△), [hmim][PF$_6$]-MFC (■) and PVDF-MFC (○).

Fig. 3 – Acetate mass transfer (k_A) and diffusion (D_A) coefficients for the different membranes.

Fig. 4 – The relationship of the energy yield (Y_S) and Coulombic efficiency (*CE)* with oxygen mass transfer coefficient of membranes separators (k_O) employed in MFCs. (○) *CE* from literature data (Table 2); Black color symbols display Y_S taken from Table 2. (♦) [bmim][NTf$_2$]-SILM; (■) Nafion N115; (▲) PVDF; (▼) [hmim][PF$_6$]-SILM.
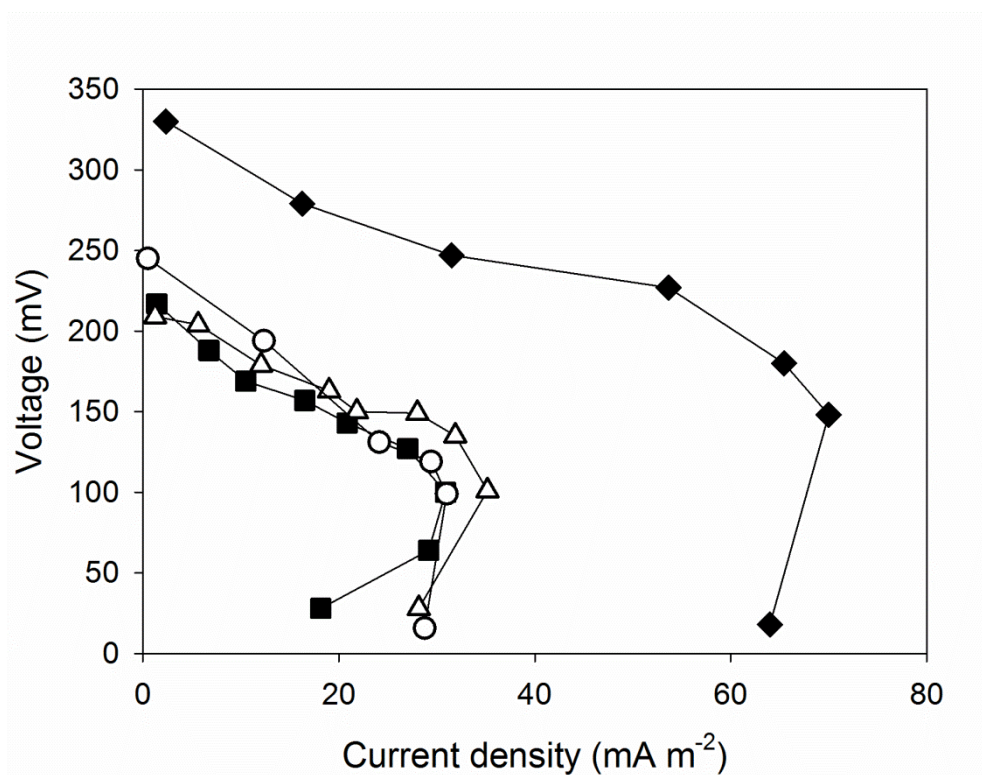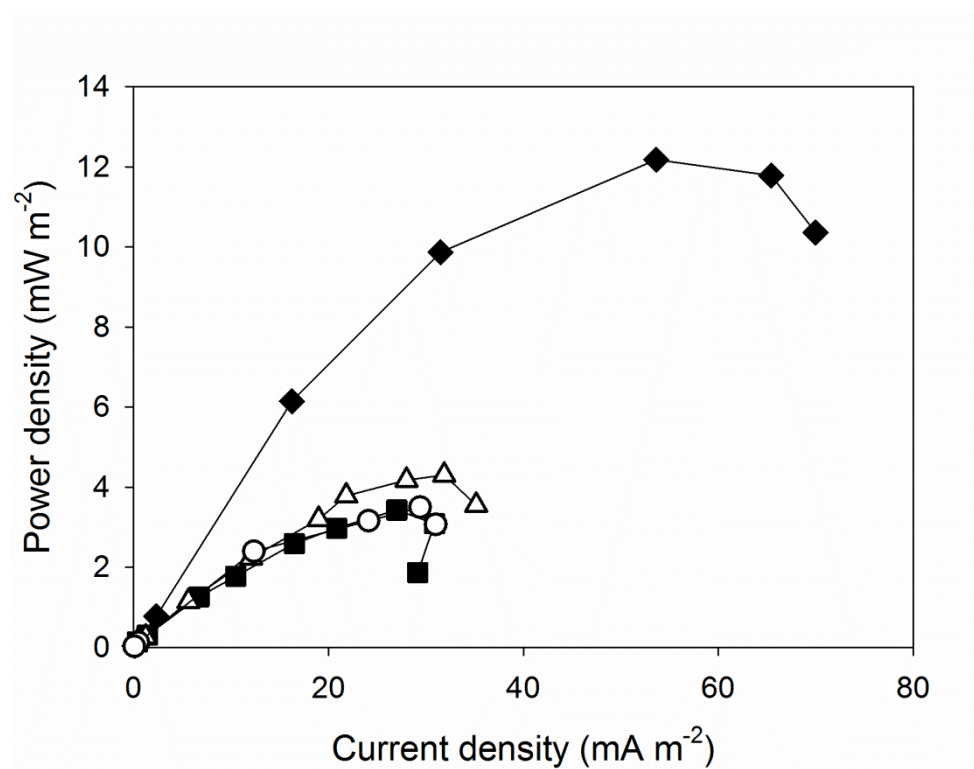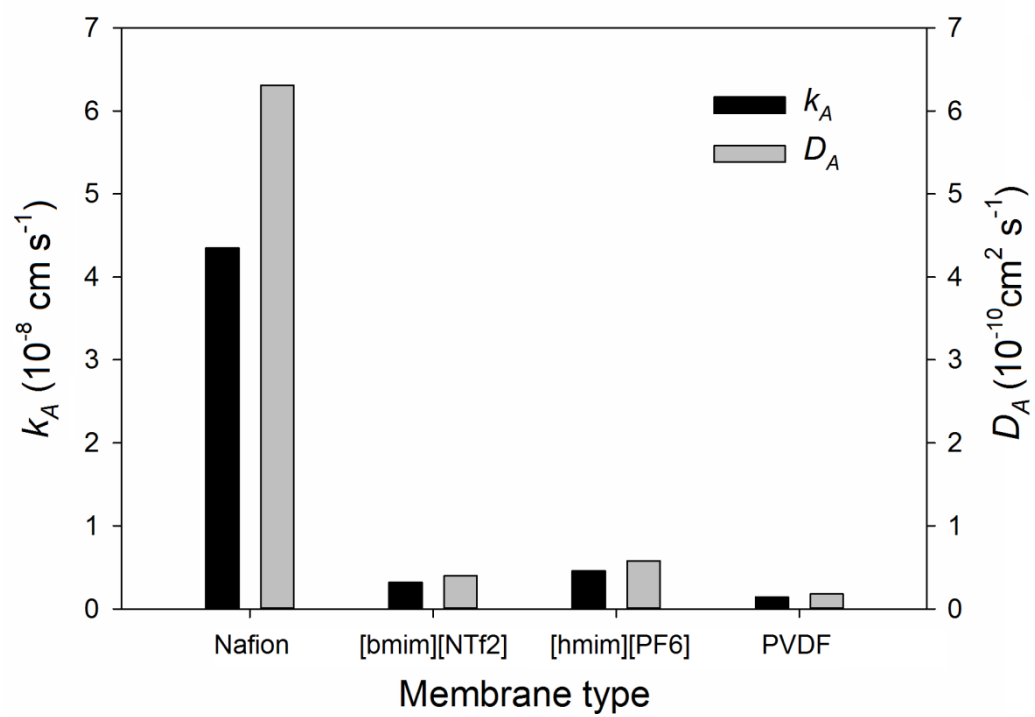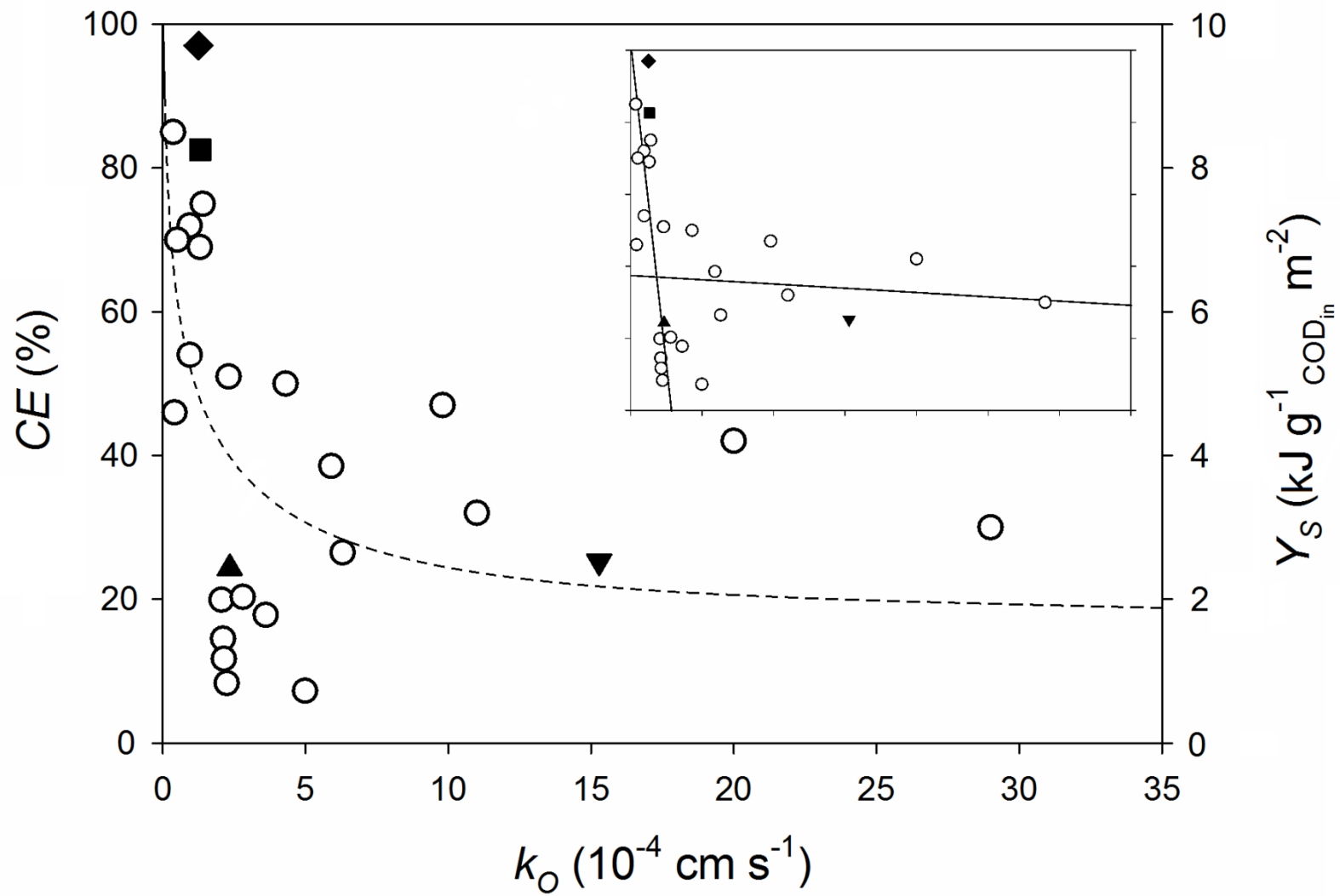
Fig. 1

Fig. 2

Fig. 3

Table 1 – Results of the polarization and permittivity measurements

4

Membrane	MFC properties		IL properties	
	R_i (kΩ)	R^2 (-)	$\tan(\delta)$ (-)	σ (mS m^{-1})
Nafion	1.36	0.944	-	-
[bmim][NTf$_2$]	2.56	0.983	0.345	283.5
[hmim][PF$_6$]	2.88	0.929	0.0319	21.8
PVDF	4.56	0.975	-	-

5

6

7

8   Table 2 – *CE* and oxygen mass transfer coefficients (k_O) for different membranes

Membrane	Membrane thickness (cm)	k_O (10^{-4} cm s^{-1})	*CE* (%)	Specifications (MFC type / anode / substrate)	Reference
Nafion	0.0175	2.3	51 ± 5	SC / carbon cloth / wastewater	[19]
SPSEBS	0.018	0.359	85 ± 7		
Nafion	0.0191	2.8	20.3	DC / carbon felt glued to stanless steel plate / 0.5 mM acetate	[15]
Nafion	0.019	2.05	19.9	Air-cathode SC / carbon paper / 100-300 mg L^{-1} Congo red, 500 mg$_{COD}$ L^{-1} glucose	[40]
UF-10k	0.04	2.24	8.3		
UF-5k	0.04	2.14	11.7		
UF-1k	0.04	2.11	14.5		
MFM	0.02	4.98	7.25		
Nafion	0.019	1.3	69	DC / carbon paper / 20 mM acetate	[21]
AEM	0.046	0.94	54 - 72		
CEM	0.046	0.94	41 - 54		
UF-1k	0.0265	0.41	38 - 49		
Nafion	0.019	4.3	50 ± 3.1	DC / carbon paper / 20 mM acetate	[20]
CEM	0.0002	9.8	47 ± 7		
Cellulose	0.00136	11	32 ± 5		
PP100	0.0045	20	42 ± 2.1		
Nafion	0.019	1.4	74.7 ± 4.6	DC / graphite rod / 10 mM acetate	[22]
MFM	0.013	5.9	38.5 ± 3.5		
Nafion	0.0145	1.31	8.25*	DC / carbon cloth / 5 mM acetate	This work
PVDF	0.0125	2.34	2.43*		
[bmim][NTf2]	0.0125	1.25	9.78*		
[hmim][PF6]	0.0125	15.28	2.52*		
Nafion	0.0178	3.6	17.8 ± 4.3	DC / carbon felt / 0.5 mM acetate	[17]
Anodisc CFM	0.00635	6.3	26.5 ± 1.9		
J-Cloth	0.03	29	30 ± 10	Air-cathode SC / carbon cloth / 1 g L^{-1} acetate	[8]
Glass fiber	0.1	0.5	70		

9   * The values are given as energy yield (Y_S, in the unit of kJ g^{-1} COD$_{in}$ m^{-2}). Abbreviations: AEM – anion exchange
10   membrane; CEM – cation exchange membrane; CFM – ceramic filtration membrane; DC – dual chamber; MFM –
11   microfiltration membrane; PP – polypropylene; SC – single chamber; SPSEBS – sulfonated polystyrene-ethylene-
12   butylene-polystyrene; UF – ultrafiltration membrane.